第 50 卷第 12 期 中国科学技术大学学报 Vol. 50, No. 12
2020 年 12 月 JOURNAL OF UNIVERSITY OF SCIENCE AND TECHNOLOGY OF CHINA Dec. 2020
Received: 2018-10-12; Revised: 2018-11-01 doi:10.3969/j.issn.0253-2778.2020.12.009

Modified Stoney formula for in-situ lithiation stress measurement in thin-film Si electrode

LIU Peilin, LU Yuyang, ZHENG Dongchang, HE Linghui, NI Yong*
CAS Key Laboratory of Mechanical Behavior and Design of Materials, Department of Modern Mechanics,
University of Science and Technology of China, Hefei 230027, China
*Corresponding author. E-mail: yni@ustc.edu.cn

Abstract: The multi-beam optical stress sensor method combined with Stoney equation is an effective approach to measure in-situ average stress in thin film electrodes upon lithiation/delithiation. However, the classic Stoney formula is applicable only at low stress states. A modified Stoney formula for stress measurement in thin-film Si electrodes was applied to account for the combined effects of the Li concentration-dependent material properties and large substrate curvature change. The numerical results based on three-dimensional non-linear finite element model for the full coupling of large deformation and Li diffusion confirm the accuracy of the modified Stoney equation. Further, a critical condition for the curvature bifurcation was discussed, which should be avoid when using the modified Stoney equation.

Keywords: modified stoney formula; finite element analysis; bifurcation; stress; plasticity; large deformation

CLC number: TU459$^+$4;O484.2 **Document code**: A

1 Introduction

Building lithium-ion battery with high energy density and large rate capability has a great market prospect to power various applications from portable electronic devices to electric vehicles[1-3]. Silicon is a particularly attractive electrode material for the lithium-ion battery because of its highest specific capacity known as 3580 mAh · g^{-1}[4], which is about 10 times the capacity of traditional graphitic carbon electrode. However, the huge expansion/contraction up to 300% during charging/discharging processes usually leads to significant lithiation stress, which results in notable mechanical damage, loss of capacity and decrease of performance in the electrodes[5-7]. Extensive efforts reported in several review papers are focused on lithiation stress evolution by developing modeling or simulation or in-situ measurement when charged and discharged[8-13].

The multi-beam optical stress sensor (MOSS) method has been proved to be a promising strategy for in-situ stress measurement in thin film-substrate systems[14]. This method uses parallel array of laser beams to detect the stress-induced substrate curvature change via a CCD camera[15], and then the average stress in the film is derived by using the Stoney formula which builds up an explicit relationship between the average substrate curvature and the average biaxial film stress[16-17]. Sethuraman et al. successfully realized real time measurement of the biaxial stress of the Si thin films using the MOSS method in a Li-ion battery half-cell[6-7,18]. Such MOSS method can not only track the in-situ stress accumulation and relaxation[18-19], but also provide an efficient approach to probe various stress-relaxation mechanisms, i. e. plasticity, fracture[23-24], diffusion-controlled creep[25], to investigate the real time change of biaxial modulus[26], stress-potential coupling[27], and rate-dependent mechano-electrochemical response[28-29] in crystalline silicon electrodes, composite silicon electrodes[30-32], composite negative-electrodes[33], germanium electrodes[24,34], Sn-based bilayer electrode[25] and etc.

Usually the classic Stoney formula adopts the assumption of small deformation and linear effect, which applies only at low stress states. On the one hand, upon lithiation/delithiation the thickness variation of the film required to accommodate the huge volume change is significant[18], and there are notable changes of material parameters for the $Li_x Si$ system as a function of state-of-charge (SOC) reported by computations and experiments[35-36]. Shenoy et al. using first-principles calculated Young's modulus softened by about an order

Citation: IU Peilin, LU Yuyang, ZHENG Dongchang, et al. Modified Stoney formula for in-situ lithiation stress measurement in thin-film Si electrode. J. Univ. Sci. Tech. China, 2020, 50(12): 1516-1524.

of magnitude compared to its original value when Si electrode is fully lithiated[35]. Experimental observations report that the biaxial moduli is reduced to about one third during lithiation[26]. On the other hand, when the substrate is thin and the internal stress in the film is large, several research groups have developed the extension of Stoney formula for large deflection to account for high-order curvature in other film-substrate systems[37-41]. A modified Stoney formula based on the bi-layer cantilever configuration has been applied to reveal how the average lithiation stress in the film varies nonlinearly with Li concentration[30-31]. Recently, many theoretical works have been devoted to studying the influences of Li concentration-dependent Young's modulus, finite deformation, and film-substrate thickness ratio on the lithiation stress in silicon electrode materials upon lithiation/delithiation[42-43]. The Li concentration-dependent material properties in the film and the presence of large substrate curvature change definitely have a significant impact on the stress development and thus challenge the validity of the classic Stoney formula. Particularly, there are even multiple solutions of the principle curvatures indicating the shape bifurcation of the substrate above a critical condition. Obviously, the validity of the classic Stoney formula for measuring the internal stress is in dispute after the one-by-one relationship between stress and curvature is destroyed[30-32].

Inspired by previous work about the extension of Stoney formula to account for high-order curvature[40], in this paper, we propose a modified Stoney formula for in-situ lithiation stress measurement in thin-film Si electrodes by taking into account the combined effects of the Li concentration-dependent material properties[35] and large substrate curvature change. Three-dimensional non-linear finite element simulation (FEM) for the full coupling of large deformation and mass diffusion in thin-film Si electrodes[44-45] is also performed to verify the accuracy of the modified Stoney equation. The results demonstrate that the average lithiation stress in the film by the classic Stoney formula is underestimated in the presence of large substrate curvature. Compared to the classic Stoney formula, our modified Stoney formula is more accurate for the thin substrate, or the film with high yield strength. A critical condition for the curvature bifurcation is also discussed when the modified Stoney equation is no longer applicable.

2 Method

The silicon film bonded to the current collector is sketched in Fig. 1(a), which can be considered as a film-substrate system. The silicon film expands during the insertion of lithium, as shown in Fig. 1(b). In this case, compressive stress is generated in the silicon film

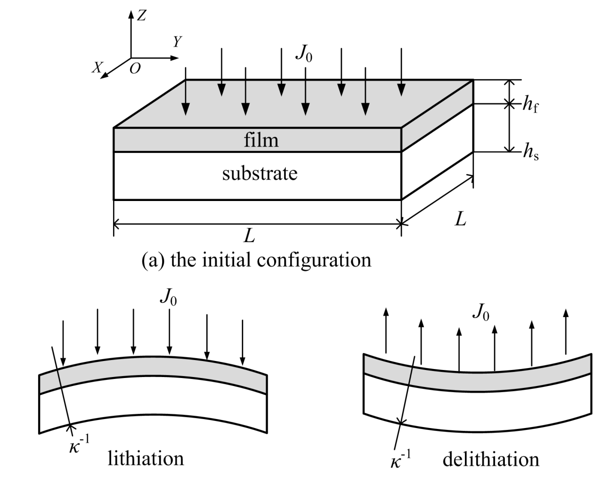

Fig. 1 Sketch of the film-substrate system subjected to a Li-ion flux on the top surface of the film.

since the expansion of the film is constrained by the substrate. In contrast, the silicon film shrinks during the extraction of lithium and tensile stress arises in the silicon film, as sketched in Fig. 1(c). The classic Stoney formula establishes the relationship between the average in-plane stress in the film and the curvature, which can be detected by the deflection of the film-substrate system via the MOSS method. The classic Stoney formula, which is written below, has been applied in the in-situ measurement of lithiation stress in lithium ion batteries.

$$\sigma_{\text{Stoney}} = \frac{E_s h_s^2 \kappa}{6h_f(1-\nu_s)} \tag{1}$$

where σ_{Stoney} is the average stress in the film, κ and h_f are the curvature and the thickness of the film, respectively. h_s, E_s and ν_s are the thickness, the Young's modulus and Poisson's ratio of the substrate, respectively.

It should be noted that the out-of-plane deflection is assumed to be small in the classic Stoney formula. However, the silicon electrode usually suffers from large elastoplastic deformation and the mechanical properties are strongly dependent on the lithium concentration during lithiation and delithiation. In this paper, we propose a modified Stoney formula relating the curvature of the film-substrate system to the average stress in the film where the geometrically nonlinear deformation cannot be neglected. To verify the accuracy of the modified Stoney formula, non-linear finite element simulation for fully coupled large deformation and mass diffusion in thin-film Si electrode has also been performed by following previous models.

2.1 Modified Stoney formula

Assuming the isotropic material properties of the film and the substrate, we adopt a modified Stoney formula considering the contribution of high-order curvature[37-41] and further incorporating the influence of concentration dependent material properties[35], to measure the stress in high-capacity film electrode material subjected to large deformation during lithiation or delithiation[40].

$$\sigma(C) \approx \sigma_{\text{Stoney}}\left\{1+4\frac{E_f(C)}{E_s}\frac{h_f(C)}{h_s}-\frac{h_f(C)}{h_s}+\frac{L^4\kappa^2}{120h_s^2(1+\nu_s)}\cdot\left[1+\left(1+\frac{1+\nu_s}{1+\nu_f(C)}\right)\frac{E_f(C)}{E_s}\frac{h_f(C)}{h_s}-\frac{h_f(C)}{h_s}\right]\right\} \tag{2}$$

where L is the lateral size of the film, for simplicity, the lateral size along X axis and Y axis is set to be $L_x = L_y = L$. C is the normalized average lithium concentration in the film. $E_f(C)$ and $\nu_f(C)$ are the concentration dependent Young's modulus and Poisson's ratio of the film, respectively, which are given by[35]

$$E_f(C) = \frac{70.9C + 90.13}{1 + 3.75C} \tag{3}$$

$$\nu_f(C) = \frac{0.9C + 0.28}{1 + 3.75C} \tag{4}$$

$h_f(C)$ is the thickness of the film after lithiation, which is related to the lithium concentration by[46]

$$h_f(C) = h_f^0(1 + 2.7C) \tag{5}$$

where h_f^0 is the thickness of the silicon film when the lithium concentration equals zero.

2.2 Finite element simulation

In order to validate the modified Stoney formula under the large-deformation condition, we perform finite element simulations for the film-substrate system shown in Fig. 1. In the finite element model, the interface between the film and substrate is assumed to be strong enough, so that the debonding of the film from the substrate can be avoided. A constant lithium-ion flux J_0 is perpendicularly applied on the top surface of the film electrode. The lithium can only diffuse in the film electrode, while, the substrate is impermeable for lithium. For the convenience of numerical simulation, a quarter of the configuration shown in Fig. 1 is selected in the finite element model, and symmetric boundary conditions are applied on the planes of *XOZ* and *YOZ*. The film and the substrate are constructed by C3D20T element and C3D8R element, respectively. Details of geometric dimensions are listed in Tab. 1.

Tab. 1 Sizes of film-substrate system used in the finite element simulation.

parameters	symbols	values
lateral size	L	20–120 mm
film thickness	h_f	0.25 μm
substrate thickness	h_s	250 μm

Tab. 2 Materials parameters for the finite element simulation.

parameters	symbols	values
density of silicon	ρ_{Si}	2.2 g · cm^{-3}[47]
expansion coefficient	β	0.5536[34]
diffusivity	D_0	1×10^{-16} m^2 · s^{-1}[46]
gas constant	R	8.314 J · mol^{-1} · K^{-1}
temperature	T	300 K
critical yield strain	ε_Y	1.56%[46]
yield stress	σ_Y	1.5 GPa[33]
Young's modulus of substrate	E_s	130 GPa[46]
Poisson's ratio of substrate	ν_s	0.26[46]

First principle calculations have demonstrated that the silicon material properties are dependent on the lithium concentration[35]. The concentration dependent Young's modulus and Poisson's ratio expressed in Eqs. (3) and (4) are adopted in the finite element model. The capacity of the silicon is 3580 mAh · g^{-1}. Moreover, the plastic deformation is taken into account. Referring to previous studies[33-34,46-47], parameters used in the finite element model are listed in Tab. 2. According to the analogy between the diffusion induced stress and the thermal stress, the stress evolution is calculated by ABAQUS thermal-stress solver[46]. The average curvatures of the film-substrate system along two orthogonal directions (x and y axes) are extracted by ABAQUS scripts.

3 Results and discussion

We can obtain the average stress in the silicon film by modified Stoney formula and finite element model. In this paper, the thickness of the film is fixed, while, we focus on the impacts of lateral size and the material property change on the evolutions of stress and curvature. First, we validate the modified Stoney formula through comparing the classic Stoney formula under small-deformation condition and the finite element model under large-deformation condition. Next, the modified Stoney formula is applied to calculate the stress evolution in the silicon film during lithiation and delithiation, which undergoes elastoplastic large deformation. Further, we calculate the stress evolution by finite element model when the bifurcation of the curvature arises in the film with large lateral size. We demonstrate that the parameters of the film-substrate system should be carefully designed in the experiment to avoid the bifurcation.

3.1 Validation of the modified Stoney formula

As mentioned above, the application of the classic Stoney formula is constrained to the small elastic deformation film-substrate system[4,15]. In this subsection, the accuracy of the modified Stoney formula is validated under both small elastic deformation and large elastic deformation conditions by the classic Stoney formula and the finite element model, respectively. The lateral size of the film is set as $L=80$ mm. The curvature of the film-substrate system is controlled by the quantity of lithium accommodated in the film electrode, which is referred to as SOC. Taking the lithiation process as an example, the curvature increases as the increasing SOC. The evolution of the average stress in the film electrode with the increasing curvature calculated by the classic Stoney formula, the modified Stoney formula and the finite element model are compared in Fig. 2. We can see that the average stress by these three methods are consistent with each other when the curvature is small ($\kappa<0.3\ \mathrm{m}^{-1}$). Note that both the modified Stoney equation and the finite element model work well when the curvature of the film becomes large ($\kappa>0.3\ \mathrm{m}^{-1}$). However, the classic Stoney formula is not applicable in this case. The reason is that the classic Stoney formula is derived based on the framework of small deformation, neglecting the effect of high order curvature.

3.2 Applications to the elastoplastic Si film electrode

The stress development in the silicon electrode attracts much attention. In the in-situ experiment for the measurement of lithiation stress, the average stress in the film is always obtained by the classic Stoney formula once the curvature of the film-substrate system is measured by the MOSS method. On the one hand, previous studies have pointed out that the silicon film electrode undergoes large elastoplastic deformation. On the other hand, first principle calculations show that the elastic modulus of the silicon electrode decreases dramatically after lithiation, which significantly affects the stress amplitude. However, the classic Stoney formula ignores these important factors. As analyzed above, the modified Stoney formula is more suitable for probing the stress evolution with the capacity for the silicon film electrode that undergoes large elastoplastic deformation during electrochemical cycling.

For the silicon film electrode with lateral size $L=100$ mm and yield stress $\sigma_Y=1.5$ GPa, the average stress in the film obtained by the classic Stoney formula, the modified Stoney formula and the finite element analysis are compared in Fig. 3. It is obvious that the average stress is underestimated by the classic Stoney formula due to the ignorance of the contribution of the high-order curvature to the stress. Once again, the accuracy of the modified Stoney formula is validated by the finite element model when the large elastoplastic deformation occurs. From this figure, we can see that the compressive stress arises during the insertion of lithium into the silicon film. The reason is that the expansion of the silicon film induced by the lithium is constrained by the substrate. At the early stage of lithiation, the compressive stress increases as the capacity increases. Then, the compressive stress gradually decreases as the lithiation proceeds after the silicon film undergoes plastic deformation. During delithiation, the lithium is extracted from the silicon film electrode, the compressive stress changes into tensile stress as the capacity decreases. At the early stage of delithiation, the tensile stress linearly increases, indicating that the silicon film undergoes elastic deformation. As the delithiation proceeds, the backward-bending part on the stress curve implies that the silicon film undergoes plastic deformation, which has been demonstrated by previous works[26-28].

The lateral size of the film electrode and the yield stress significantly affect the curvature and the stress amplitude in the film, which are investigated in Fig. 4. When the lateral size of the film is reduced to 20 mm and the yield stress is maintained as 1.5 GPa, the curves

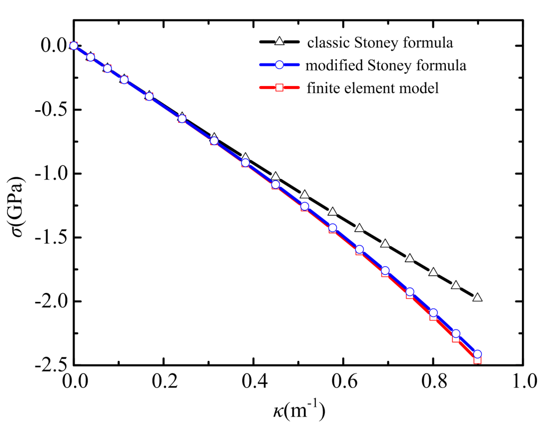

Fig. 2 Comparison of the average stress evolution with the curvature of the film-substrate system obtained by the classic Stoney formula.

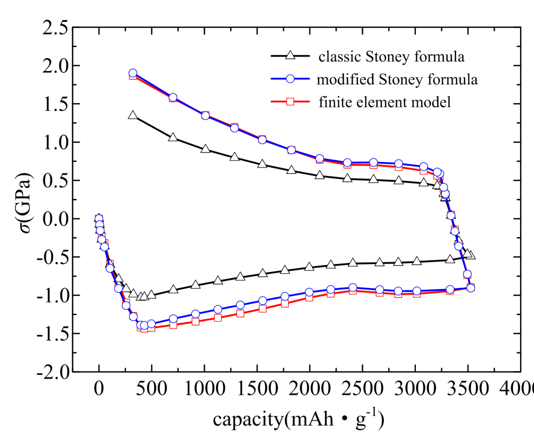

Fig. 3 Comparison of the stress evolution with the capacity among the classic Stoney formula, the modified Stoney formula and the finite element analysis for elastoplastic Si film electrode during lithiation and delithiation.

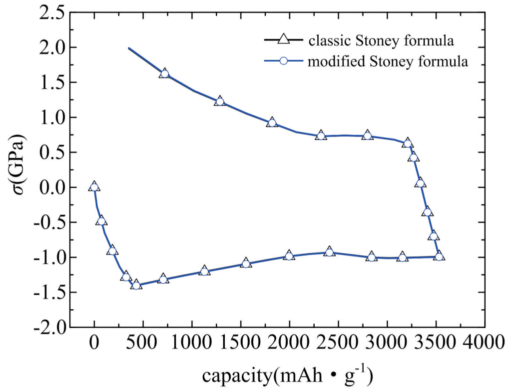

(a) small lateral size L=20 mm and high yield stress σ_Y = 1.5 GPa

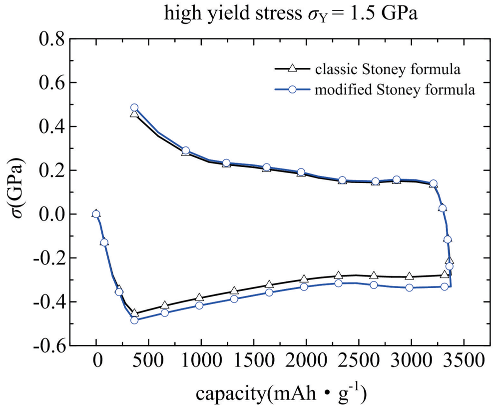

(b) large lateral size L=100 mm and low yield stress σ_Y = 0.5 GPa

Fig. 4 Effects of the lateral size (L) and yield stress (σ_Y) on the average stress evolution in the film with the capacity during lithiation and delithiation.

for the average stress evolution with the capacity obtained by the classic Stoney formula and the modified Stoney formula are plotted in Fig. 4(a). We can see that the difference between these two curves is unobvious due to the small curvature change after lithiation in the film electrode with small size. When the yield stress is reduced to 0.5 GPa and the film size is maintained as L = 100 mm, the curves for the stress evolution with the capacity by the classic Stoney formula and the modified Stoney formula are also plotted in Fig. 4(b). The small yield stress leads to the low level of stress in the film electrode. Consequently, the curvature is small and the stress-capacity curves calculated by the classic Stoney formula and the modified Stoney formula nearly collapse. We can demonstrate that both the classic Stoney formula and the modified Stoney formula work well when the lateral size or yield stress is small. However, the modified Stoney formula is more suitable when the lateral size or the yield stress is small.

In the above computational studies, the curvature is obtained by FEM simulations. For in-situ lithiation-stress measurement of thin-film Si electrode, the curvature is derived by using the MOSS method. As shown in Fig. 5, we built a similar apparatus composed of electrochemical cell, electrochemical workstation and real-time stress measurement by following the work of Sethuraman et al.[26-28]. The electrochemical cell was assembled in an argon-filled glove box (LABstar, MBRAUN, Germany) maintained at 25 ℃ and less than 1 ppm of O_2 and H_2O. The electrodes were separated by a special holder which ensured that there was a path for lithium-ion, and neither the anode nor the cathode would contact each other. The substrate of the working electrode was Si wafers (20 mm diameter, 500 μm

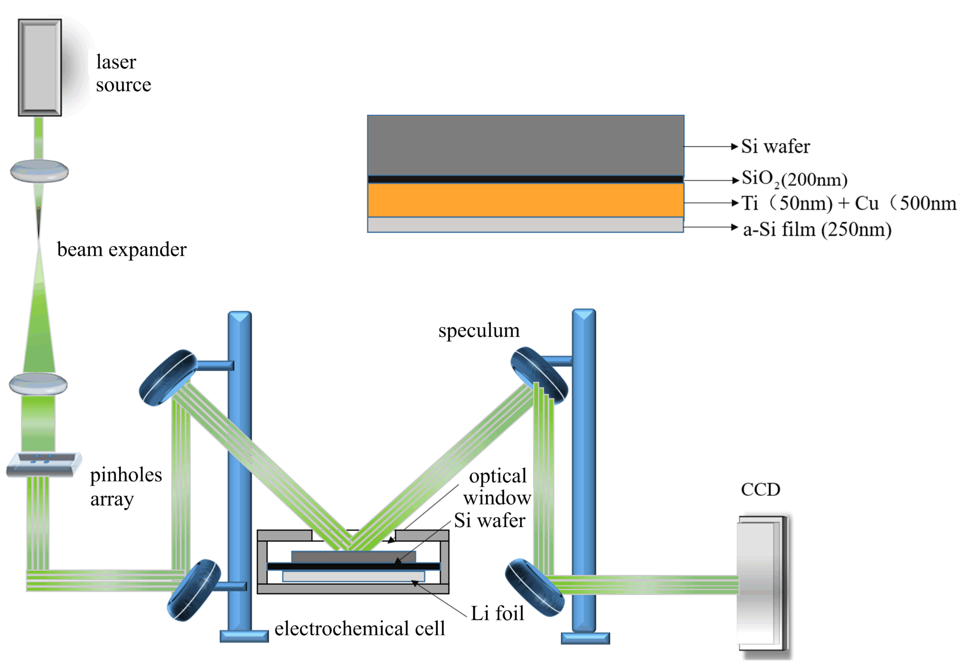

Fig. 5 Sketch of the MOSS apparatus.

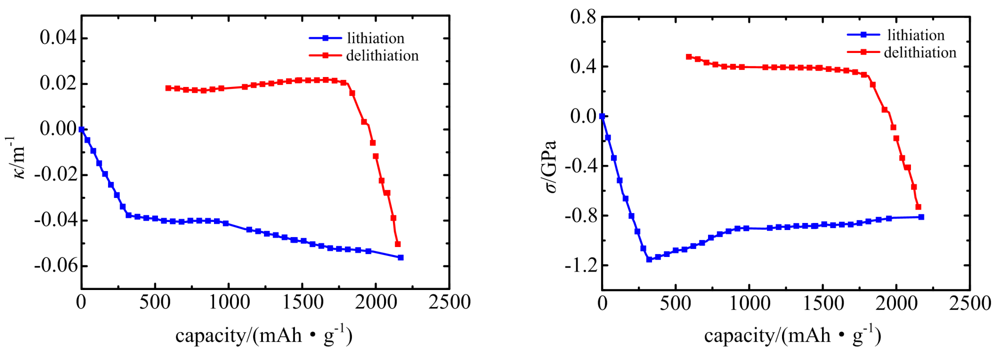

(a) measured curvature as a function of the capacity (b) calculated stress as a function of the capacity

Fig. 6 Measurement of the curvature by in-situ experiment and corresponding calculated average stress of the film electrode.

thickness, (111) orientation), one side of which was polished and the other side was coated by SiO_2 with the thickness 200 nm. The oxide layer protects the Si wafer from participating in the electrochemical reactions. An adhesion layer Ti with the thickness 50 nm, together with the current collector Cu with the thickness 500 nm, was sputtered onto the unpolished side of the Si wafer via e-beam evaporation technique under ultra-high vacuum ($< \sim 1\times10^{-6}$ Torr). Then, the working film electrode (amorphous silicon) with the thickness 250 nm was deposited by RF-magnetron sputtering at 180 W power and less than 2 mTorr Ar pressure (Lesker PVD Lab-18, Kurt Lesker Company, USA).

The electrochemical performance of the cell was controlled and measured by electrochemical workstation (ZENNIUM E, ZAHNER Scientific Instruments, Germany). The cell was cycled galvanostatically at a current of 12.5 μA · cm^{-2} (ca. C/8 rate) between 1.2 and 0.01 V vs Li/Li^+. The laser source (MGL-III-532, CNI, China) in conjunction with a collimating system performs as a beam expander and an array of pinholes generates a parallel array of laser beams. The diameter of the pinhole is 200 μm. These multiple beams are reflected off the sample surface and captured on a CCD camera (PL-D734, PixeLINK, Canada). The relative change in the laser-spot spacing on the CCD camera's sensor is related to the wafer curvature κ, through $\kappa = (d - d^0)/(dA_m)$. Here d is the distance between two adjacent laser spots on the CCD camera. d^0 is the initial distance. The mirror constant A_m is measured by placing two reference mirrors of known curvature in the sample plane and measuring the relative change in the spot spacing of the two situations. A_m is measured as 0.203 m.

As θ which is the incident angle of the laser beam on the wafer substrate is set as 30°, the optical path length of the multiple beams between the plane of the wafer substrate and CCD sensor. According to Ref. [14], $L^{opt} = A_m \cos(\theta)/2$ and is calculated as 2.13 m, and the measurement sensitivity of the system λ can be determined by $\lambda = (\delta d/d)\cos\theta/(2L^{opt})$. Here, δd is the minimum change of d, which is 5.5 μm in the CCD. d is manufactured as 400 μm. Hence, the measurement sensitivity of the system λ is calculated as 0.00258 m^{-1}. Fig. 6(a) shows the measured curvature change as a function of the capacity during lithiation and delithiation. Subsequently, we can substitute the value of the measured curvature into the modified Stoney formula in Eq. (2) to obtain the in-situ lithiation stress as a function of the capacity, as shown in Fig. 6(b).

3.3 Curvature bifurcation

Under certain conditions, the curvature of the film-substrate system along the X direction and Y direction may be unequal, which is referred to as the bifurcation of curvature[37]. In this case, both the classic Stoney formula and the modified Stoney formula are no longer applicable. The bifurcation of curvature brings difficulty to the measurement of the film deflection during lithiation/delithiation. It is worthy determining the critical curvature and stress for bifurcation, which can guide the reasonable design of the film size to avoid the bifurcation. For the silicon film electrode, the concentration dependent material properties and the film size may play important roles in the critical curvature for bifurcation. Motivated by previous studies[37], we adopt the analytical solution for bifurcation curvature by assuming the homogeneously distributed lithium in the film electrode[40],

$$\kappa_c = \pm\frac{h_s}{L^2}\sqrt{120(1-v_s)\left\{1+\left[\frac{3(1-v_s)}{1-v_f(C)}-1\right]\frac{1+v_s}{1+v_f(C)}\frac{E_f(C)}{E_s}\frac{h_f(C)}{h_s}\right\}} \tag{6}$$

Correspondingly, the critical average stress for bifurcation is given by[40]

$$\sigma_c = \frac{2E_s h_s^2}{6(1-v_s)h_f(C)}\frac{\kappa_c}{1+v_s} \tag{7}$$

When the average stress is smaller than the critical stress $\sigma < \sigma_c$, the curvatures along two directions are equal $\kappa_x = \kappa_y$. While, when the average stress exceeds the critical stress, the curvatures along two directions are no longer equal.

Although the critical curvature and stress for bifurcation are derived analytically, the stress development in the film after the bifurcation needs to be solved numerically by the finite element model. For the film electrode with the lateral size $L = 100$ mm, the curvatures along X axis and Y axis as a function of the average stress are plotted in Fig. 7. We can see that the two curvatures are equal when the average stress is small (AB range). At the critical point (B), the configuration becomes unstable and the bifurcation of curvature arises, leading to the two different curvatures along two directions as the average stress increases. In this case, both the classic Stoney formula and the modified Stoney formula are not suitable. It should be pointed out that the critical stress obtained by finite element model is a little larger than the analytical solution. The reason is that the concentration in the film is assumed to be homogeneous when deriving the analytical solution. In the finite element model, the concentration distribution is governed by the diffusion equation, leading to the inhomogeneous distribution of concentration in the silicon film.

The bifurcation behavior is significantly affected by the yield stress of the film electrode. For the film electrode with the size $L = 120$ mm, the curvatures of the electrode film along two directions versus the capacity under different yield stresses are plotted in Fig. 8. For the yield stress $\sigma_Y = 1.0$ GPa and $\sigma_Y = 1.5$ GPa, the bifurcation occurs at the critical curverature. As the yield stress decreases, the corresponding capcity increases when the bifurcation arises, suggesting that the bifurcation can be delayed with low yield stress. When the yield stress is reduced to $\sigma_Y = 0.5$ GPa, the bifurcation can be avoided even the film electrode is

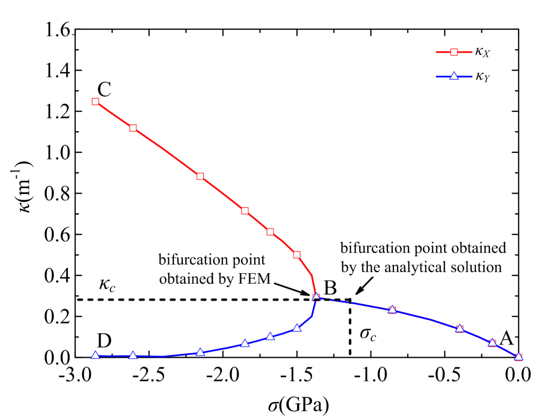

Fig. 7 Bifurcation of the curvature along the X axis and Y axis as the stress in the film increases.

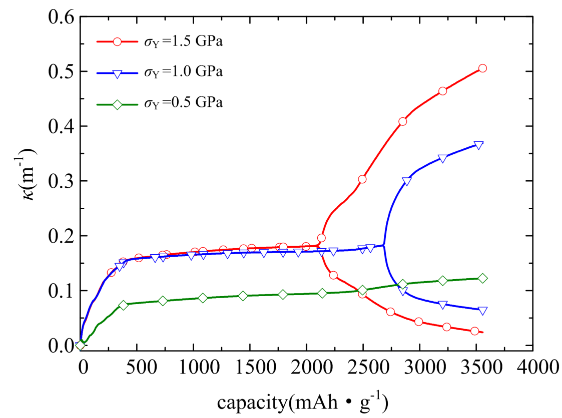

Fig. 8 Effect of yield stress on the bifurcation behavior of the film electrode with the lateral size $L = 120$ mm.

fully lithiated. Note that the level of stress is limited by the yield stress and the configuration of the film is stable under the small stress. That is why the bifurcation of the film is retarded under the small yield stress.

4 Conclusions

In this paper, the modified Stoney formula is applied to establish the relationship between the average stress and the curvature of the silicon film electrode, taking into account the effects of high-order curvature and concentration-dependent material properties. The modified Stoney formula is validated by the classic Stoney formula under the small elastic deformation condition and the finite element model under the large elastoplastic deformation condition. We point out that the modified Stoney formula is more suitable when the lateral size or the yield stress is large. However, the modified Stoney equation is not applicable when the bifurcation of the film curvature arises. In this case, we analytically derive the critical curvature and average stress for bifurcation. Further, the transformation of stable deformation to the bifurcation is simulated by the finite element model. We demonstrate that the large yield stress and large film size facilitate the bifurcation. Thus, the film size should be reasonable designed by finite element model to avoid the bifurcation before performing in-situ measurement of the lithiation stress in the film electrode. In the future, we will measure the average stress in various promising high capacity film electrode, including the sulfur film electrode and graphite-silicon composite electrode, where the stress measurement is desirable and the stress can play an important role on the electrode performance.

In the future, we will measure the average stress in various promising high capacity film electrode, including the sulfur film electrode and graphite-silicon composite electrode, where the stress measurement is desirable and the stress can play an important role on the electrode performance.

Acknowledgments

The work is supported by the National Natural Science Foundation of China (11672285), the Strategic Priority Research Program of the Chinese Academy of Sciences (XDB22040502), China Postdoctoral Science Foundation (2018M642532), the Fundamental Research Funds for the Central Universities (WK2090050046), the Collaborative Innovation Center of Suzhou Nano Science and Technology, and the Fundamental Research Funds for the Central Universities.

Conflict of interest

The authors declare no conflict of interest.

Author information

LIU Peilin is a master student under the supervision of Prof. Ni Yong at University of Science and Technology of China (USTC). She received her bachelor's degree in Engineering Mechanics from North China University of Water Conservancy and Hydropower in 2014. Her research mainly focuses on the in-situ measurement of lithiation stress in thin-film Si electrode.

NI Yong (corresponding author) is a Professor of Mechanics at University of Science and Technology of China (USTC). He received his B. S. degree in Theoretical and Applied Mechanics in 2000 and Ph. D. degree in Solid Mechanics in 2004, both from USTC. From 2005 to 2009, he worked in Hong Kong University, National Institute of Standard and Technology, and Rutgers University as a visiting scholar and Research Associate, respectively. He joined the USTC faculty as a Professor of Mechanics in 2009. His research mainly focuses on mechanics of microstructured materials.

References

[1] Chiang Y M. Building a better battery. Science, 2010, 330(6010): 1485-1486.

[2] Goodenough J B, Kim Y. Challenges for rechargeable Li batteries. Chemistry of Materials, 2009, 22(3): 587-603.

[3] Tarascon J M, Armand M. Issues and challenges facing rechargeable lithium batteries. Nature, 2001, 414(6861): 359-367.

[4] Li H, Huang X, Chen L, et al. A high capacity nano Si composite anode material for lithium rechargeable batteries. Electrochemical and Solid-State Letters, 1999, 2(11): 547-549.

[5] Mukhopadhyay A, Sheldon B W. Deformation and stress in electrode materials for Li-ion batteries. Progress in Materials Science, 2014, 63: 58-116.

[6] Chan C K, Peng H, Liu G, et al. High-performance lithium battery anodes using siliconnanowires. Nature Nanotechnology, 2008, 3(1): 31-35.

[7] Dahn J R, Zheng T, Liu Y, et al. Mechanisms for lithium insertion in carbonaceous materials. Science, 1995, 270(5236): 590-593.

[8] Zhang S. Chemomechanical modeling of lithiation-induced failure in high-volume-change electrode materials for lithium ion batteries. npj Computational Materials, 2017, 3(1): 7.

[9] Zhang S, Zhao K, Zhu T, et al. Electrochemomechanical degradation of high-capacity battery electrode materials. Progress in Materials Science, 2017, 89: 479-521.

[10] Xu R, Zhao K. Electrochemomechanics ofelectrodes in Li-ion batteries: A review. Journal of Electrochemical Energy Conversion and Storage, 2016, 13(3): 030803.

[11] Gao Y, Cho M, Zhou M. Mechanical reliability of alloy-based electrode materials for rechargeable Li-ion batteries. Journal of Mechanical Science and Technology, 2013, 27(5): 1205-1224.

[12] Mcdowell M T, Xia S, Zhu T. The mechanics of large-volume-change transformations in high-capacity battery materials. Extreme Mechanics Letters, 2016, 9: 480-494.

[13] Lu Y Y, NI Y. Stress-mediated lithiation in nanoscale phase transformation electrodes. Acta Mechanica Solida Sinica, 2017, 30(3): 248-253.

[14] Chason E, Sheldon B. Monitoring stress in thin films during processing. Surface Engineering, 2003, 19(5): 387-391.

[15] Floro J, Chason E, Lee S, et al. Real-time stress evolution during $Si_{1-x}Ge_x$ heteroepitaxy: Dislocations, islanding, and segregation. Journal of Electronic Materials, 1997, 26(9): 969-979.

[16] Stoney G G. The tension of metallic films deposited by electrolysis. Proc. R. Soc. Lond. A, 1909, 82(553): 172-175.

[17] Chason E, Guduru P R. Tutorial: Understanding residual stress in polycrystalline thin films through real-time measurements and physical models. Journal of Applied Physics, 2016, 119(19): 191101.

[18] Sethuraman V A, Chon M J, Shimshak M, et al. In-situ measurements of stress evolution in silicon thin films during electrochemical lithiation and delithiation. Journal of Power Sources, 2010, 195(15): 5062-5066.

[19] Brown J J, Lee S H, Xiao J, et al. Observations of stress accumulation and relaxation in solid-state lithiation and delithiation of suspended Si microcantilevers. Physica Status Solidi A, 2016, 213(8): 2156-2168.

[20] Nadimpalli S P, Sethuraman V A, Bucci G, et al. On plastic deformation and fracture in Si films during electrochemical lithiation/delithiation cycling. Journal of The Electrochemical Society, 2013, 160(10): A1885-A1893.

[21] Lu Y Y, Ni Y. Effects of particle shape and concurrent plasticity on stress generation during lithiation in particulate Li-ion battery electrodes. Mechanics of Materials, 2015, 91: 372-381.

[22] Chang L, Lu Y, He L, et al. Phase field model for two-phase lithiation in an arbitrarily shaped elastoplastic electrode particle under galvanostatic and potentiostatic operations. International Journal of Solids and Structures, 2018, 143: 73-83.

[23] Chon M J, Sethuraman V A, Mccormick A, et al. Real-time measurement of stress and damage evolution during initial lithiation of crystalline silicon. Physical Review Letters, 2011, 107(4): 045503.

[24] Pharr M, Choi Y S, Lee D, et al. Measurements of stress and fracture in germanium electrodes of lithium-ion batteries during electrochemical lithiation and delithiation. Journal of Power Sources, 2016, 304: 164-169.

[25] Lu Y, Che Q, Song X, et al. Stress self-relaxation arising from diffusion-induced creep in bilayer lithium-ion battery electrode. Scripta Materialia, 2018, 150: 164-167.

[26] Sethuraman V A, Chon M J, Shimshak M, et al. In-situ

measurement of biaxial modulus of Si anode for Li-ion batteries. Electrochemistry Communications, 2010, 12 (11): 1614-1617.
[27] Sethuraman V A, Srinivasan V, Bower A F, et al. In-situ measurements of stress-potential coupling in lithiated silicon. Journal of The Electrochemical Society, 2010, 157 (11): A1253-A1261.
[28] Sethuraman V A, Srinivasan V, Newman J. Analysis of electrochemical lithiation and delithiation kinetics in silicon. Journal ofThe Electrochemical Society, 2013, 160 (2): A394-A403.
[29] Tavassol H, Jones E M, Sottos N R, et al. Electrochemical stiffness in lithium-ion batteries. NatureMaterials, 2016, 15 (11): 1182.
[30] Li D, Wang Y, Hu J, et al. In-situ measurement of mechanical property and stress evolution in a composite silicon electrode. Journal of Power Sources, 2017, 366: 80-85.
[31] Xie H, Zhang Q, Song H, et al. Modeling and in situ characterization of lithiation-induced stress in electrodes during the coupled mechano-electro-chemical process. Journal of Power Sources, 2017, 342: 896-903.
[32] Li D, Wang Y, Hu J, et al. Role of polymeric binders on mechanical behavior and cracking resistance of silicon composite electrodes during electrochemical cycling. Journal of Power Sources, 2018, 387: 9-15.
[33] Sethuraman V A, Van Winkle N, Abraham D P, et al. Real-time stress measurements in lithium-ion battery negative-electrodes. Journal of Power Sources, 2012, 206: 334-342.
[34] NADIMPALLI S P, TRIPURANENI R, SETHURAMAN V A. Real-time stress measurements in germanium thin film electrodes during electrochemical lithiation/delithiation cycling. Journal of The Electrochemical Society, 2015, 162 (14): A2840-A2846.
[35] Shenoy V B, Johari P, Qi Y. Elastic softening of amorphous and crystalline Li-Si phases with increasing Li concentration: A first-principles study. Journal of Power Sources, 2010, 195(19): 6825-6830.
[36] Qi Y, Hector L G, James C, et al. Lithium concentration dependent elastic properties of battery electrode materials from first principles calculations. Journal of The Electrochemical Society, 2014, 161(11): F3010-F3018.
[37] Mézin A. Coating internal stress measurement through the curvature method: A geometry-based criterion delimiting the relevance of Stoney's formula. Surface and Coatings Technology, 2006, 200: 5259-5267.
[38] Harper B D, Chih-ping W. A geometrically nonlinear model for predicting the intrinsic film stress by the bending-plate method. International Journal of Solids and Structures, 1990, 26: 511-525.
[39] Masters C B, Salamon N. Geometrically nonlinear stress-deflection relations for thin film/substrate systems. International Journal of Engineering Science, 1993, 31(6): 915-925.
[40] Fahnline D, Masters C B, Salamon N. Thin film stress from nonspherical substrate bending measurements. Journal of Vacuum Science & Technology A: Vacuum, Surfaces, and Films, 1991, 9(4): 2483-2487.
[41] Freund L. Substrate curvature due to thin film mismatch strain in the nonlinear deformation range. Journal of the Mechanics and Physics of Solids, 2000, 48: 1159-1174.
[42] Wen J, Wei Y, Cheng Y T. Examining the validity of Stoney-equation for in-situ stress measurements in thin film electrodes using a large-deformation finite-element procedure. Journal of Power Sources, 2018, 387: 126-134.
[43] Lu Y, Chang L, Yao H, et al. Transition from deceleration to acceleration of lithiation front movement in hollow phase transformation electrodes. Journal of The Electrochemical Society, 2017, 164(13): A3371-A3379.
[44] Bower A F, Guduru P R, Sethuraman V A. A finite strain model of stress, diffusion, plastic flow, and electrochemical reactions in a lithium-ion half-cell. Journal of the Mechanics and Physics of Solids, 2011, 59(4): 804-828.
[45] Bower A F, Guduru P. A simple finite element model of diffusion, finite deformation, plasticity and fracture in lithium ion insertion electrode materials. Modelling and Simulation in Materials Science and Engineering, 2012, 20 (4): 045004.
[46] An Y, Jiang H. A finite element simulation on transient large deformation and mass diffusion in electrodes for lithium ion batteries. Modelling and Simulation in Materials Science and Engineering, 2013, 21(7): 074007.
[47] Renner O, Zemek J. Density of amorphous silicon films. Czechoslovak Journal of Physics, 1973, 23 (11): 1273-1276.

应用修正 Stoney 公式原位测量硅薄膜电极中的锂化应力

刘佩琳,陆宇阳,郑东昌,何陵辉,倪勇*

中国科学院材料力学行为和设计重点实验室,中国科学技术大学近代力学系,安徽合肥 230027

摘要:结合 Stoney 公式的多光臂应力测量方法能够有效检测出薄膜电极在充放电过程中的平均应力.然而,经典 Stoney 公式仅适用于低应力水平的情况.运用修正的 Stoney 公式考虑了硅电极材料力学性质的变化和基底曲率剧烈变化情况下电极薄膜中应力的演化规律.基于应力和扩散相互耦合的三维非线性有限元模型,验证了修正 Stoney 公式的准确性.进一步,讨论了曲率分叉出现的条件,确保使用修正的 Stoney 公式时避免出现曲率分叉行为.

关键词:修正 Stoney 公式;有限元;分叉;应力;塑性;大变形